Biogeosciences Discuss., 9, 9425–9451, 2012
www.biogeosciences-discuss.net/9/9425/2012/
doi:10.5194/bgd-9-9425-2012

Biogeosciences Discussions

A model-based constraint of CO_2 fertilisation

P. B. Holden[1], N. R. Edwards[1], D. Gerten[2], and S. Schaphoff[2]

[1]Environment, Earth and Ecosystems, Open University, Milton Keynes, UK
[2]Potsdam Institute for Climate Impact Research, Potsdam, Germany

Received: 18 July 2012 – Accepted: 19 July 2012 – Published: 27 July 2012

Correspondence to: P. B. Holden (p.b.holden@open.ac.uk)

Published by Copernicus Publications on behalf of the European Geosciences Union.

Abstract

We derive a constraint on the strength of CO_2 fertilisation of the terrestrial biosphere through a "top-down" approach, calibrating Earth System Model parameters constrained only by the post-industrial increase of atmospheric CO_2 concentration. We derive a probabilistic prediction for the globally averaged strength of CO_2 fertilisation in nature, implicitly net of other limiting factors such as nutrient availability. The approach yields an estimate that is independent of CO_2 enrichment experiments and so provides a new constraint that can in principal be combined with data-driven priors. To achieve this, an essential requirement was the incorporation of a Land Use Change (LUC) scheme into the GENIE earth system model, which we describe in full. Using output from a 671-member ensemble of transient GENIE simulations we build an emulator of the change in atmospheric CO_2 concentration change over the preindustrial period (1850 to 2000). We use this emulator to sample the 28-dimensional input parameter space. A Bayesian calibration of the emulator output suggests that the increase in Gross Primary Productivity in response of a doubling of CO_2 from preindustrial values is likely to lie in the range 11 to 53 %, with a most likely value of 28 %. The present-day land-atmosphere flux (1990–2000) is estimated at $-0.6\,\mathrm{GTC\,yr^{-1}}$ (likely in the range 0.9 to $-2.0\,\mathrm{GTC\,yr^{-1}}$). The present-day land-ocean flux (1990–2000) is estimated at $-2.2\,\mathrm{GTC\,yr^{-1}}$ (likely in the range -1.6 to $-2.8\,\mathrm{GTC\,yr^{-1}}$). We estimate cumulative net land emissions over the post-industrial period (land use change emissions net of the CO_2 fertilisation sink) to be 37 GTC, likely to lie in the range 130 to -20 GTC.

1 Introduction

Experimental evidence almost univocally shows a stimulation of leaf photosynthesis when plants are exposed to elevated CO_2 (Koerner, 2006). In addition to this direct effect on photosynthesis, the short time-scale physiological effect of reduced stomatal opening increases water-use efficiency and additionally increases the efficiency of

BGD
9, 9425–9451, 2012

photosynthesis (Field et al., 1995). The combined effects, which we group under the label of CO_2 fertilisation, act as a negative feedback for anthropogenic carbon emissions. Increased concentrations of atmospheric CO_2 lead to increased photosynthesis and more efficient drawdown, transferring some fraction of these emissions from the atmosphere into terrestrial carbon pools. However, the strength of the fertilisation effect is poorly quantified, especially under natural conditions. Some studies have failed to detect a measurable effect in nature, while others suggest that any effects may be short term as CO_2 is only one of a number of potentially limiting factors on plant growth (Koerner, 2006). In addition to the implications for future vegetation and crop growth, improved quantification of the globally integrated effects of CO_2 fertilisation in nature is crucial to reduce the uncertainties in carbon-cycle predictions from process-based models. In response to SRES A2 forcing, predictions of 2100 CO_2 from 11 C^4MIP models ranged from 740 to 1030 ppm, the largest source of uncertainty coming from the terrestrial response to elevated CO_2 (Friedlingstein et al., 2006).

The concept of CO_2 fertilisation has been well demonstrated in many studies under controlled conditions. The most extensive of these experiments applied the FACE (free-air CO_2 enrichment) approach to both coniferous and deciduous trees in four separate sites (Norby et al., 2005). This study measured a 23 % increase of NPP following a doubling from preindustrial CO_2 concentrations. However, there remains doubt as to whether the effect is realised under natural conditions as a result, for instance, of nitrogen limitation (Norby et al., 2010) or temperature limitation in Boreal forest (Hickler et al., 2008). Girardin et al. (2011) failed to measure an effect in boreal forest, setting an upper limit on the CO_2 fertilisation effect at the detection limit, estimated at 14 %. In a model-based study of the period 1973–2004, the inclusion of nitrogen limitation was found to reduce the strength of the global carbon-cycle feedback to just 27 % of that with only carbon cycling (Bonan and Levis, 2010). Quantification is made even more difficult because elevated CO_2 levels are associated with increased temperatures, increasing respiration rates and opposing any change due to fertilisation. Hickler et al. (2008) validated the dynamic vegetation model LPJ-GUESS (Smith et al., 2001)

BGD
9, 9425–9451, 2012

against the FACE experiments of Norby et al. (2005) and applied the model to a global simulation that simulated substantial regional differences in the response of forests to a CO_2 doubling, ranging from a 15 % increase in NPP in Boreal forests to a 35 % increase in tropical forests. Over a thousand scientific articles have been published on the topic, yet there is no clear consensus (Koerner et al., 2006). In short, it is far from straightforward to extrapolate empirical evidence from controlled experiments to the global scale.

We here address, for the first time, a quantification of the CO_2 fertilisation effect through a "top-down" approach. In order to achieve this we have incorporated a representation of land use change into the intermediate complexity earth system model GENIE; emissions from land use change constitute a substantial (and poorly quantified) source of anthropogenic emissions. We perform a 671-member ensemble of simulations with GENIE. We use these simulations to build an emulator of atmospheric CO_2 concentration that we apply to probe the high dimensional parameter space more fully. We then apply Bayesian calibration to emulator outputs in order to constrain CO_2 fertilisation by calibrating vegetation parameters against observed CO_2. The reduced complexity of GENIE is ideal for performing the large number of simulations required for such an analysis. All vegetation is treated as a single plant functional type that responds to the changing CO_2 concentration in the same way. Thus, in effect, we are constraining the global average plant response to describe observational data. Whilst GENIE is relatively crude, it has some notable advantages over more complex models for this purpose. A "bottom-up" modelling approach, accounting for multiple plant functional types and spatially variable nutrient availability and soil characteristics is itself subject to substantial uncertainties which, largely due to computational limitations, are extremely challenging to quantify in a probabilistic sense.

BGD
9, 9425–9451, 2012

2 GENIE and the implementation of land use change

We apply the coupled carbon cycle-climate model GENIE. The physical model (Marsh et al., 2011) comprises the 3-D frictional geostrophic ocean model GOLDSTEIN (at $36 \times 36 \times 16$ resolution) coupled to a 2-D Energy Moisture Balance Atmosphere and a thermodynamic-dynamic sea-ice model. Vegetation is simulated with ENTS, a dynamic model of terrestrial carbon storage (Williamson et al., 2006). Ocean chemistry is modelled with BIOGEM (Ridgwell et al., 2007) and is coupled to the sediment model SEDGEM at 36×36 resolution (Ridgwell and Hargreaves, 2007). More detail of the specific model configuration can be found in Holden et al. (2012).

In order to perform this experiment, the major extension required to ENTS was an implementation of land use change (LUC) effects on the carbon cycle and climate. We call this revised model ENTSmL. For the modelling of LUC, each grid cell is apportioned between natural vegetation and cultivated vegetation. No distinction is made between crop and pasture. We adapt the ENTS formulation (Williamson et al., 2006) to describe the vegetation state within a grid cell with two state variables C_{vN} (the natural vegetation carbon density) and C_{sT} (the total soil carbon density, averaged over both natural and cropped regions). The vegetative carbon density in cultivated regions is defined to be zero, equivalent to the simplifying assumption that cultivated vegetation is either negligible (pastures) or is continually harvested and instantly released to the atmosphere (crops).

In ENTSmL, natural vegetative carbon density is given by

$$dC_{vN}/dt = P - R_v - L \quad (1)$$

where the expressions providing the rates P (photosynthesis), R_V (vegetation respiration) and L (leaf litter) are unchanged from the ENTS formulation (Williamson et al., 2006). We do not repeat these equations here, but briefly summarise their dependencies. Photosynthesis is a function of CO_2, soil moisture, air temperature and fractional vegetation cover. Leaf litter is linearly related to C_{vN} and, via a function designed

BGD
9, 9425–9451, 2012

to represent self-shading, to NPP. Vegetation respiration depends exponentially upon temperature. Parameters are varied in each of these components (base photosynthesis rate k18, CO_2 fertilisation rate k14 ("VPC"), the fractional vegetation dependence upon vegetative carbon density k17, base leaf litter rate k26 and temperature dependence of plant respiration k20). Although the expression for CO_2 fertilisation parameterises the uncertain saturating increase in Gross Primary Production under elevated CO_2, the simplified moisture balance formulation does not capture the changes in evapotranspiration, soil moisture and run-off due to the physiological effect (Leipprand and Gerten, 2006, Betts et al., 2007).

In ENTSmL, soil carbon density is defined as the average over both natural and cultivated regions. In naturally vegetated regions, the rate of change of soil carbon density is given by

$$dC_{sN}/dt = L - R_s \quad (2)$$

where the temperature-dependent soil respiration rate R_s is given by Williamson et al. (2006). The parameter dominating the uncertainty in the temperature dependence (k32) is varied across the ensemble.

Harvesting reduces the carbon returned to the soil in arable regions. This loss of soil carbon may be aggravated due to agricultural processes such as tillage, which increases oxidation rates. Arable soils are predicted to be losing carbon in all European countries at an estimated average rate of $70\,\mathrm{g\,C\,m^{-2}\,yr^{-1}}$ (Janssens et al., 2005). To capture this effect in ENTSmL, the leaf litter input to the soil in cultivated regions is derived from the natural leaf litter rate, reduced by a fraction k_C. Previous modelling studies have applied a similar parameterisation. Olofsson and Hickler (2010) applied a 33 % reduction, Stocker et al. (2011) applied a 43 % reduction. Here, k_C is a variable parameter in the ensemble, distributed uniformly between 0 (leaf litter input to the soil is unchanged from the natural rate) and 1 (no leaf litter input to soils in cultivated regions). The rate of change of soil carbon density in cultivated regions is thus given by

$$dC_{sC}/dt = (1 - k_C)L - R_s \quad (3)$$

BGD
9, 9425–9451, 2012

The rate of change of soil carbon is the weighted average of these two terms

$$dC_{sT}/dt = (1 - f_C)(L - R_s) + f_C\{(1 - k_C)L - R_s\} \tag{4}$$

where f_C is the grid cell fraction under cultivation (a prescribed forcing that is both temporally and spatially variable, see Sect. 3). This simplifies to

$$dC_{sT}/dt = (1 - f_C k_C)L - R_s \tag{5}$$

When cultivated areas are expanded we assume that 50 % of the cleared carbon is released immediately to the atmosphere. The remaining 50 % is added to the soil carbon reservoir where it respires on timescales that are dependent upon the local climate. The model of Stocker et al. (2011) releases 25 % directly to the atmosphere, with the remainder split evenly into two pools that decay on timescales of 2 and 20 yr. These authors concluded that the assessment of LUC emissions on decadal or longer timescales was not sensitive to these values. Although ENTS has only one soil carbon pool, we capture the uncertainty in the decay rate of cleared carbon through the ensemble parameter k32 (Williamson et al., 2006) that controls the temperature dependence of respiration. To illustrate the range of variability, at 15 °C, the approximate global average temperature, the ensemble spread in k32 produces respiration decay timescales of 11 to 25 yr. We note that shrinking cultivated regions are modelled analogously so that vegetative carbon is instantaneously returned to natural values, 50 % of the carbon coming from the soil and 50 % from the atmosphere. On the global scales relevant to this model this approximation appears reasonable, especially as rates of deforestation dominate over reforestation throughout the historical period. Reforested regions attain 50 % of natural terrestrial carbon storage instantly, with the remainder accumulating over time as the soil carbon pool is restored to equilibrium values.

We model the climatic impacts of LUC through its effect on surface albedo and roughness length. (The soil moisture bucket implementation is unchanged but bucket capacity is affected by LUC due to altered soil carbon.) We note that although modelled soil carbon is generally reduced under LUC as a consequence of the reduced efficiency

BGD
9, 9425–9451, 2012

of soil creation (k_C parameterisation above), increases can be simulated due to the climatic impacts of LUC, for instance, via increased albedo that creates local cooling and reduced respiration rates.

In cultivated regions that are not snow covered, albedo is assumed equal to α_C, an ensemble parameter that is allowed to vary in the range 0.12 to 0.18 (parameter ALUA in Table 1). The selection of this range is based upon values estimated for various crops (Hansen, 1993). The albedo in natural regions α_N is calculated as a function of local vegetative and soil carbon density, using the standard ENTS expression (Williamson et al., 2006). The albedo of the grid cell is a weighted average of the two

$$\alpha_C = (1 - f_C)\alpha_N + f_C\alpha_C \quad (6)$$

Snow-covered albedo and local climate are strongly dependent upon the nature of the local vegetation (Betts, 2000). Rather than introducing an additional parameter, we capture the increased albedo of snow-covered deforested regions with the ENTS expression applied to the (reduced) average vegetative carbon density across the gridcell $(1 - f_C)C_{vN}$. Roughness length is derived similarly, by applying the average vegetative carbon density to the standard ENTS expression.

3 Ensemble design

A 671-member ensemble of transient simulations was performed, varying 28 key model parameters. Twenty-four of the parameters were previously calibrated to produce an ensemble of 471 plausible preindustrial "spin-up" simulations corresponding to 471 points in the 28-dimensional input space (Holden et al., 2012). These 24 parameters were selected for their importance to the carbon cycle, either directly or indirectly through their role on climate and ocean dynamics. Four additional (uncalibrated) parameters were added for the transient experiment described here (Table 1). Two of these parameters (KC and ALUA) represent uncertain processes in the new LUC implementation (Sect. 3). A third, OL1 describes the uncertain outgoing longwave

BGD
9, 9425–9451, 2012

radiation response to changes in radiation forcing (Holden et al., 2010). The ranges for this parameter were based on an earlier calibration (Holden et al., 2010) which produced a climate sensitivity distribution of 2.4 to 5.1 °C (90 % confidence). Finally, VPC describes the uncertain response of photosynthesis to changing CO_2 concentrations, parameter k14 in Williamson et al. (2006).

These four additional parameters were added in a series of four maximin latin hypercube designs, summarised in Table 1. Experiments 1, 3 and 4 were 100-member ensembles with the same randomly selected sub-sample of the 471-member spin-ups. Experiment 2 was performed on the remaining 371 spin-ups. Experiments 3 and 4 were performed in order to better calibrate the tails of the VPC distribution, regions that exert the greatest leverage upon the subsequent emulations and calibration (Sect. 4). Experiment 1 applied a more conservative range for ALUA, a range that produced a globally-averaged LUC radiative forcing from ~ 0.2 to 0.5 W m^{-2} in a single parameter sweep.

Each transient simulation continues from the relevant spin-up simulation and runs from AD1 to AD 2005, with boundary conditions held fixed for the first 850 yr to allow a correction for any drift due to minor inconsistencies with the spin-up boundary conditions. Simulations were forced with CMIP5 fossil fuel CO_2 emissions (including cement and gas flaring) from 1751 to 2005, http://cmip-pcmdi.llnl.gov/cmip5/forcing.html#CO2-emissions. Other forcings (850 to 2005) – land use change, solar variability, orbital configuration, non-CO2 trace gases, direct aerosol effects and volcanic forcing – are described in Eby et al. (2012). In the GENIE implementation of these forcings, a globally uniform perturbation to the radiative forcing is added to reflect non-CO2 trace gases, the direct aerosol effect and volcanic forcing.

The Land Use Change data set applied was PMIP3 data (800 to 1699, Pongratz et al., 2007) linearly blended over the period 1500 to 1699 with the CMIP5 historical RCP land use data (1500 to 2005, Hurtt et al., 2011). This combined dataset (Eby et al., 2012) provides fractional coverage of crops and pasture at annual resolution and at

BGD
9, 9425–9451, 2012

0.5° degree spatial resolution. The crop and pasture data were summed and integrated (retaining the annual resolution) onto the ∼ 10° GENIE grid.

4 Methods

The flow chart (Fig. 1) summarises the methodology. The ensemble displayed a wide range of responses, with ensemble-averaged terrestrial carbon loss over the period 1850 to 2000 of 128 ± 139 GTC (1σ uncertainties are provided throughout). This compares to estimates of ∼ 100 to 120 GTC from the range of LUC scenarios considered by Stocker et al. (2011), neglecting their illustrative scenario of a linear scaling of fractional LUC from 10 000 BC to present day. Note that Stocker et al. (2011) considered LUC scenario uncertainty rather than parametric uncertainty. This comparison suggests that parametric uncertainty (∼ 100 GTC) dominates over LUC uncertainty (∼ 10 GTC), so that our neglect of the latter is reasonable. We note that 123 of the GENIE simulations exhibited an increase in terrestrial carbon storage over this period. Although the direct consequences of LUC can only reduce terrestrial carbon in the model (through reductions in vegetation density and in the leaf litter-rate to soils), the effects of carbon emissions (CO_2 fertilisation and climate) and indirect (climate-driven) LUC feedbacks, acting upon both natural and cultivated vegetation, can combine to increase the modelled global terrestrial carbon reservoir.

In order to calibrate the model response we apply the constraint of ΔCO_2, the simulated increase in atmospheric CO_2 from 1850 to 2000. This constraint is ideal for vegetation calibration as it is associated with a negligible observational error, but exhibits a wide range of simulated values across the ensemble (117 ± 41 ppm, cf. the observed increase of 90 ppm). It is important to note that the ensemble variability is dominated by two of the poorly constrained terrestrial vegetation and land-use change parameters: 41 % of the variance in ΔCO_2 is captured by a linear dependence on VPC and 28 % by a linear dependence on KC. The ensemble variability due to all other 26 parameters together generate an uncertainty of ∼ 16ppm, compared to VPC and KC, which together contribute ∼ 38ppm. For this reason, we only consider the calibration of these two parameters. The remaining 26 parameters cannot be further calibrated by this constraint, in general because they have already been constrained by the requirement for preindustrial plausibility. It should also be emphasised, however, that these 26 parameters do contribute to significant uncertainty across the ensemble that, together with inherent structural error, limit the degree to which CO_2 fertilisation can be constrained. We note that the calibration of VPC described here is independent of the preindustrial precalibration as the parameterisation is normalised to unity when $CO_2 = 280$ ppm.

We choose to constrain on the basis of ΔCO_2 rather than present-day CO_2 as we are here concerned with the response of the system to changing CO_2 and this approach avoids additional uncertainty due to an imperfect prediction of the preindustrial state. We prefer to avoid the alternative approach of tightly constraining by preindustrial CO_2 as this would contradict our ensemble design philosophy which is to rule out only those simulations which are un-controversially implausible, necessary (Edwards et al., 2011) for the Bayesian calibration which follows. We note that ensemble-averaged preindustrial CO_2 (280 ± 15 ppm) is well centred on observations. The variability can be largely attributed to ∼centennial-scale instabilities that are apparent in ∼ 30 % of the simulations, which appear to be related to the presence of alternative stable states, likely driven by ocean convection and/or stratification-dependent mixing. We choose not to filter out these simulations, in part as it was found to be very difficult to distinguish the instability from natural variability with an objective test. Imposing (somewhat subjective) tests to eliminate stability was not found to have a significant effect on the emulation and calibration that follows, but including all simulations provides a more conservative (weak) constraint as it captures the complete range of ensemble variability.

It is not appropriate to derive marginal probability distributions for the two parameters without first considering their joint probability distribution, especially given the strong dependencies of ΔCO_2 on both of these parameters which leads to strong correlations between the parameters in plausible parameter space. In order to generate sufficient data to adequately sample the 28-dimensional input space, we first build an

BGD
9, 9425–9451, 2012

emulator of ΔCO_2, building on Edwards et al. (2011) who used an emulator to identify implausible regions of input parameter space. We take the 28 parameters as emulator inputs and construct a cubic emulator following a similar procedure to that described in Holden et al. (2010). A quadratic emulator was first built, allowing cross terms between all 28 parameters, to which we allow the addition of cubic terms before applying the Bayes Information Criterion (BIC) to reduce the model size. The additional cubic terms considered were the 4 cubic terms that were generated by an investigative emulation that allowed all possible cubic terms but considered only the 16 significant parameters in the quadratic model. This approach was taken to substantially improve the efficiency of the process relative to an approach that considers all possible cubic terms from 28 model parameters. Two cubic terms were retained after application of BIC (VPC^3 and AHD^*VPC^2, where AHD is atmospheric heat diffusivity). The resulting emulator fits the simulated data well, with an R^2 of 95 %.

We then designed a 14 100-member parameter set to apply as input to this emulator. The design reproduces the 470 simulated parameter sets (omitting a single parameter set which did not complete in the ensemble) thirty times, replacing the four transient parameters with a 4 × 14 100 matrix of randomly generated inputs across the ranges in Table 1. The output of this emulated ensemble is compared with the simulated ensemble in Fig. 2, illustrated by the marginal dependencies on VPC and KC. The response to changes in these parameters is well captured by the emulator. Although the most extreme values of ΔCO_2 are underestimated by the smooth polynomial functions, the emulated ensemble distribution of 114 ± 39 ppm compares favourably to the simulated distribution (117 ± 41 ppm), suggesting this reduction in variance is unlikely to be significant.

To derive a joint probability distribution we first generate a two-dimensional data bin. We subdivide the KC/VPC parameter space into 10 × 10 bins, linearly spaced for KC and quadratically spaced for VPC, across the ranges of their prior distributions (Table 1). Within each of the 10 × 10 bins we calculate the mean μ_{ij} and standard deviation σ_{ij} of simulated ΔCO_2. Within each bin the variance is dominated by uncertainty

BGD
9, 9425–9451, 2012

Title Page
Abstract | Introduction
Conclusions | References
Tables | Figures
◀| |▶
◀ ▶
Back | Close
Full Screen / Esc
Printer-friendly Version
Interactive Discussion

due the remaining 26 ensemble parameters as, to first order, VPC and KC are fixed. We apply Bayes' theorem to the bin statistics to derive a posterior distribution for each bin. Analogously to Rougier (2007), we apply

$$p(\theta_{ij}|\Delta CO_2{=}90\,\text{ppm}) = c\varphi(90\,\text{ppm}, \mu_{ij} + \mu_\varepsilon, \sqrt{\{\sigma_{ij}^2 + \sigma_\varepsilon^2\}})p(\theta_{ij}) \tag{7}$$

where φ describes a normal distribution, evaluated at 90 ppm with mean $\mu_{ij} + \mu_\varepsilon$ and standard deviation $\sqrt{(\sigma_{ij}^2 + \sigma_\varepsilon^2)}$. μ_ε and σ_ε are model structural bias and structural error respectively. c is a normalising constant. θ_{ij} are the binned values of the VPC/KC parameter pair, and $p(\theta_{ij})$ the prior probability we assign to that combination. In this application, the resulting pdf was found to be insensitive to the application of a more complex calibration procedure that explicitly integrated over the individual outputs of emulated ensemble (i.e. rather than approximating emulator output with a binned normal distribution).

It is essential to include estimates of structural error and bias in a model calibration to avoid over-constraining the resulting pdf. We derive an estimate for structural error by applying the approach of Murphy et al. (2007) who suggest the inter-model spread of a quantity provides some measure because it reflects, at least in part, different structural choices that can be made. Although such an approach is likely to provide an underestimate because different models likely share some sources of structural error, it is conservative in the sense that a component of the inter-model variability will arise from parametric uncertainty (but be attributed to structural error). C^4MIP simulations forced by SRES A2 exhibit a standard deviation of 90 ppm in the simulated increase in CO_2 in 2100 relative to 2000 (Friedlingstein et al., 2006). We note that this study found no systematic differences between the behaviours of OAGCMs and EMICs. We linearly scale the C^4MIP inter-model variability by the relative increase in CO_2 in the two experiments to estimate a ΔCO_2 structural error of ± 17 ppm.

In our LUC implementation, a potentially significant source of structural bias is the assumption that vegetative carbon is negligible in cultivated regions, leading to excess simulated LUC emissions. In order to quantify this neglect, we performed a simulation

BGD
9, 9425–9451, 2012

A model-based constraint of CO_2 fertilisation

P. B. Holden et al.

with the global crop and vegetation model LPJmL (Bondeau et al., 2007). We ran the model with the current land use data of Fader et al. (2010) that prescribes the crop distribution of the individual crop functional type as an annual fraction of the grid cell. Above ground biomass of the cropland area (1.5 Mha) was averaged over the growing season, with sowing dates calculated after Waha et al. (2012). Biomass on the set aside area, represented by grass, grows between the cropping season. The time-weighted mean of crop and set-aside biomass gives the average above ground biomass estimation of the cropland area. Managed grassland (2.7 Mha) is grown over the entire year and is harvested whenever the increment of net primary production (NPP) exceeds 300 gC m^{-1}. Cropland and managed grassland are combined to yield an estimated global above-ground LUC biomass of 3 GTC. In order to convert this to a structural bias in atmospheric CO_2 concentration, we apply the ensemble relationship between ΔCO_2 and total emissions T (time integrated fossil fuel emissions and terrestrial carbon change) which is well described by $\Delta CO_2 = 0.2887\,T$ ($R^2 = 92\,\%$). This relationship suggests that our neglect of the carbon stored in above-ground LUC biomass leads to an over-estimation of ΔCO_2 by ~ 1 ppm which can reasonably be neglected in the calibration ($\mu_\varepsilon = 0$ ppm).

In order to apply pre-calibration and investigate the full range of model responses we allowed very high values of KC (Eq. 3, Table 1). These high values (leading to high loss of soil carbon under LUC) can, in general, only be reconciled with compensating high rates of CO_2 fertilisation. However, very high values of KC are not physically reasonable. Most notably, KC is applied to all cultivated regions (crop and pasture) whereas the effect of reduced leaf litter efficiency is only likely to be relevant to crop regions. The global apportionment of ~ 50 : 50 crop: pasture alone places an upper bound on KC to be ~ 0.5. This value for an upper bound is itself unreasonable at it implies total loss of soil carbon in cropped regions. We thus apply a prior assumption for KC, $p(\theta_{ij}) = \varphi$ (KC, 0.2, 0.1). The maximum likelihood of the prior is influenced by previous modelling studies with tuned LUC models (Olofsson and Hickler, 2008; Stocker et al., 2011), which suggest a 40 % reduction of leaf-litter input to arable soils, approximately equivalent to KC = 0.2 applied to all cultivated regions. We assume this prior is normally distributed with a standard deviation of 0.1. We do not apply a prior for VPC in order to ensure that the posterior is independent of data-based estimates of CO_2 fertilisation.

5 Results

We apply Eq. (7) to derive the joint probability distributions for KC and VPC illustrated in Fig. 3. In these plots, VPC is re-expressed as the percentage increase in photosynthesis in response to a doubling of CO_2 from preindustrial levels. This facilitates comparison with alternative modelling implementations and data-based estimates. Figure 3a applies a uniform prior, Fig. 3b constrains the loss in arable soil carbon to more reasonable values by applying the KC prior (Sect. 4). In both plots, structural error of σ_ε = 17 ppm and structural bias μ_ε = 0 ppm are applied (Sect. 4). The comparison is provided to demonstrate the important role played by the KC prior. The calibration provides little constraint on the upper bound of VPC if all values of KC are allowed because unreasonably high soil carbon losses (KC → 1) can be reconciled with high values of VPC.

We integrate over the joint distribution in Fig. 3b to derive the marginal probability distribution for VPC, plotted as the blue curve in Fig. 4. This base case analysis implies a most likely CO_2 fertilisation effect of 28 %, likely in the range 11 % to 53 %. The influence of the structural error assumption is illustrated by the red curve in Fig. 4, which is calculated with σ_ε = 0 ppm. The calculation suggests a much stronger constraint on VPC, but one which cannot be justified as it is equivalent to assuming that the only model uncertainty is due to uncertainty in the input parameters.

Figure 5a plots the calibrated distribution of post-industrial terrestrial carbon change, calculated as the probability-weighted integration of the simulated change (2000–1850). The KC prior and the VPC posterior are combined to derive the probability weighting for each simulation. This analysis predicts a 66 % probability that the change in terrestrial biomass lies between a loss of 130 GTC and a gain of 20 GTC. The

BGD
9, 9425–9451, 2012

probability-weighted mean of 37 GTC provides a best estimate of net post-industrial LUC emissions, consistent with data-driven estimates (for the period 1800 to 1994) of 39 ± 28 GTC (Sabine et al., 2004). Note that the estimated total emissions T = 315 GTC (including prescribed fossil fuel emissions of 278 GTC) are consistent with the simple estimate implied by the linear fit derived earlier: $T \approx \Delta CO_2/0.2887 = 312$ GTC, demonstrating internal consistency of the analysis.

Figure 5b illustrates a similar analysis applied to calibrate the land-atmosphere carbon flux over the recent period (1990 to 2000) with a probability-weighted mean of −0.6 GTC yr^{-1} and a 66 % confidence interval of uncertain sign, ranging from −2.0 to 0.9 GTC yr^{-1}. Figure 5c illustrates the ocean-atmosphere flux, with a probability weighted mean of −2.2 GTC yr^{-1} and a 66 % confidence interval in the range −1.6 to −2.8 GTC yr^{-1}. These figures compare with IPCC estimates (Denman et al., 2007) of a land-atmosphere flux (1990 to 2000) of −1.0 ± 0.6 GTC yr^{-1} and an ocean-atmosphere flux of −2.2 ± 0.4 GTC yr^{-1}. More recently, Le Quéré et al. (2009) estimated LUC emissions (1990 to 2005) of 1.5 ± 0.7 GTC yr^{-1} offset by a terrestrial sink (1990 to 2000) of 2.6 ± 0.7 GTC yr^{-1}, implying a net land-atmosphere flux of −1.1 ± 1.0 GTC yr^{-1}, and estimated an ocean-atmosphere flux of −2.2 ± 0.4 GTC yr^{-1}.

6 Summary and conclusions

We have incorporated a relatively simple implementation of LUC into ENTS, the dynamic terrestrial carbon module of GENIE, and applied the model in an attempt to constrain the response of terrestrial vegetation to increased atmospheric CO_2. The resulting probability distribution for GPP increase in response to doubled CO_2 suggests a significant effect in the range 11 to 53 %, with a most likely value of 28 %. Although the uncertainty is substantial, unsurprising in view of well-known difficulties in constraining the terrestrial carbon cycle, the result is useful for two reasons. Firstly, the analysis is by definition a calibration of the fertilisation effect net of other limiting factors, providing a globally averaged vegetation response that is balances the carbon budget. Secondly,

BGD
9, 9425–9451, 2012

the approach does not impose a data-based constraint on the strength of CO_2 fertilisation, other than to assume its possible existence. As such, the calibrated distribution provides a useful independent constraint that can be used in conjunction with existing estimates. A negligible fertilisation effect appears difficult to reconcile with this analysis although, given the conservatively large estimates of parametric and structural error that appear prudent at this stage, the possibility of a negligible effect cannot be ruled out. Additional data-based constraints, such as the isotopic composition of atmospheric CO_2, may enable a more constrained calibration in the future. Although the approach cannot capture the regionally disparate responses that are apparent in more complex models (Hickler et al., 2008) it nevertheless provides a useful global constraint. This may be especially useful for application to complex vegetation models that are not coupled to global models of the carbon cycle. The estimate of post-industrial carbon loss, in particular the quantification of uncertainty – likely in the range 130 to −20 GTC – may provide a useful constraint on post-industrial terrestrial emissions in order to ensure that they are consistent with the relatively well constrained estimates of fossil fuel emissions and ocean uptake.

Acknowledgements. We acknowledge support from EU FP7 ERMITAGE grant no. 265170.

References

Betts, R. A.: Offset of the potential carbon sink from boreal reforestation by decreases in surface albedo, Nature, 408, 187–190, 2000.

Betts, R. A., Boucher, O., Collins, M., Cox, P. M., Falloon, P. D., Gedney, N., Hemming, D. L., Huntingford, C., Jones, C. D., Sexton, D. M. H., and Webb, M. J: Projected increase in continental runoff due to plant responses to increasing carbon dioxide, Nature, 448, 1037–1042, doi:10.1038/nature06045, 2007

Bonan, G. B. and Levis, S.: Quantifying carbon-nitrogen feedbacks in the Community Land Model (CLM4), Geophys. Res. Lett., 37, L07401, doi:10.1029/2010GL042430, 2010.

Bondeau, A., Smith, P. C., Zaehle, S., Schaphoff, S., Lucht, W., Cramer, W., Gerten, D., Lotze-Campen, H., Müller, C., Reichstein, M., and Smith, B.: Modelling the role of agriculture

for the 20th century global terrestrial carbon balance, Glob. Change Biol., 13, 679–706, doi:10.1111/j.1365-2486.2006.01305.x, 2007.
Denman, K. L., Brasseur, G., Chidthaisong, A., Ciais, P., Cox, P. M., Dickinson, R. E., Hauglustaine, D., Heinze, C., Holland, E., Jacob, D., Lohmann, U., Ramachandran, S., da Silva Dias, P. L., Wofsy, S. C., and Zhang, X.: Couplings between changes in the climate system and biogeochemistry, in: Climate Change 2007: The Physical Science Basis, Contribution of Working Group I to the Fourth Assessment Report of the Intergovernmental Panel on Climate Change, edited by: Solomon, S., Qin, D., Manning, M., Chen, Z., Marquis, M., Averyt, K. B., Tignor, M., and Miller, H. L., Cambridge University Press, Cambridge, UK and New York, USA, 2007.
Eby, M., Weaver, A. J., Alexander, K., Zickfeld, K., Abe-Ouchi, A., Cimatoribus, A. A., Crespin, E., Drijfhout, S. S., Edwards, N. R., Eliseev, A. V., Feulner, G., Fichefet, T., Forest, C. E., Goosse, H., Holden, P. B., Joos, F., Kawamiya, M., Kicklighter, D., Kienert, H., Matsumoto, K., Mokhov, I. I., Monier, E., Olsen, S. M., Pedersen, J. O. P., Perrette, M., Philippon-Berthier, G., Ridgwell, A., Schlosser, A., Schneider von Deimling, T., Shaffer, G., Smith, R., Spahni, R., Sokolov, A. P., Steinacher, M., Tachiiri, K., Tokos, K., Yoshimori, M., Zeng, N., and Zhao, F: Historical and idealized climate model experiments: and EMIC intercomparison, in preparation, 2012.
Edwards, N. R., Cameron, D. and Rougier, J.: Precalibrating an intermediate complexity climate model, Clim. Dynam., 37, 1469–1482, doi:10.1007/s00382-010-0921-0, 2011.
Fader, M., Rost, S., Müller, C., Bondeau, A., and Gerten, A.: Virtual water content of temperate cereals and maize: Present and potential future patterns, J. Hydrol., 384, 218–231, doi:10.1016/j.jhydrol.2009.12.011, 2010.
Field, C. B., Jackson, R. B., and Mooney, H. A.: Stomatal responses to increased CO_2: implications from the plant to the global scale, Plant Cell Environ., 18, 1214–1225, 1995.
Friedlingstein, P., Cox, P., Betts, R., Bopp, L., von Bloh, W., Brovkin, V., Cadule, P., Doney, S., Eby, M., Fung, I., Bala, G., John, J., Jones, C., Joos, F., Kato, F., Kawamiya, M., Knorr, W., Lindsay, K., Matthews, H. D., Raddatz, T., Rayner, P., Reick, C., Roeckner, E., Schnitzler, K.-G., Schnur, R., Strassman, K., Weaver, A. J. Yoshikawa, C., and Zeng, N.: Climate-carbon cycle feedback analysis: results from the C^4MIP model intercomparison, J. Climate, 19, 3337–3353, doi:10.1175/JCLI3800.1, 2006.

BGD
9, 9425–9451, 2012

A model-based constraint of CO_2 fertilisation

P. B. Holden et al.

Girardin, M. P., Bernier, P. Y., Raulier, F., Tardif, J. C., Conciatori, F., and Guo, X. J.: Testing for a CO_2 fertilisation effect on growth of Canadian boreal forests, J. Geophys. Res., 116, G01012, doi:10.1029/2010JG001287, 2011.

Hansen, F. V.: Albedos, US Army Research Laboratory Report number ARL-TR-57, 1993.

Hickler, T., Smith, B., Prentice, I. C., Mjöfors, K., Miller, P., Arneth, A., and Sykes, M. Y.: CO_2 fertilisation in temperate FACE experiments not representative of boreal and tropical forests, Glob. Change Biol., 14, 1531–1542, doi:10.1111/j.1365-2486.2008.01598.x, 2008.

Holden, P. B., Edwards, N. R., Oliver, K. I. C., Lenton, T. M., and Wilkinson, R. D.: A probabilistic calibration of climate sensitivity and terrestrial carbon change in GENIE-1, Clim. Dynam., 35, 785–806, doi:10.1007/s00382-009-0630-8, 2010.

Holden, P. B., De'ath, R. M., Edwards, N. R., Müller, S. A., Oliver, K. I. C., and Ridgwell, A.: Simulated uncertainties in the spatial distribution of ocean δ^{13}C, in preparation, 2012.

Hurtt, G. C., Chini, L. P., Frolking, S., Betts, R. A., Feddema, J., Fischer, G., Fisk, J. P., Hibbard, K., Houghton, R. A., Janetos, A., Jones, C. D., Kindermann, G., Kinoshita, T., Klein Goldewijk, K., Riahi, K., Shevliakova, E., Smith, S., Stehfest, E., Thomson, A., Thornton, P., van Vuuren, D. P., and Wang, Y. P.: Harmonization of land-use scenarios for the period 1500–2100: 600 years of global gridded annual land-use transitions, wood harvest, and resulting secondary lands, Climatic Change, 109, 117–161, doi:10.1007/s10584-011-0153-2, 2011.

Janssens, I. A., Freibauer, A., Schlamadinger, B., Ceulemans, R., Ciais, P., Dolman, A. J., Heimann, M., Nabuurs, G.-J., Smith, P., Valentini, R., and Schulze, E.-D.: The carbon budget of terrestrial ecosystems at country-scale – a European case study, Biogeosciences, 2, 15–26, doi:10.5194/bg-2-15-2005, 2005.

Koerner, C.: Plant CO_2 responses: an issue of definition, time and resource supply, New Phytologist, 172, 393–411, doi:10.1111/j.1469-8137.2006.01886.x, 2006.

Le Quéré, C., Raupach, M. R., Canadell, J. G., Marland, G., Bopp, L., Ciais, P., Conway, T. J., Doney, S. C., Feely, R. A., Foster, P., Friedlingstein, P., Gurney, K., Houghton, R. A., House, J. I., Huntingford, C., Levy, P. E. Lomas, M. R., Majkut, J., Metzl, N., Ometto, J. P., Peters, G. P., Prentice, I. C., Randerson, J.T., Running, S. W., Sarmiento, J. L., Schuster, U., Sitch, S., Takahashi, T., Viovy, N., van der Werf, G. R. and Woodward, F. I.: Trends in the sources and sinks of carbon dioxide, Nat. Geosci., 2, 831–836, doi:10.1038/ngeo689, 2009.

Leipprand, A. and Gerten, D.: Global effects of doubled atmospheric CO_2 content on evapotranspiration, soil moisture and runoff under potential vegetation, Hydrol. Sci., 51, 171–185, doi:10.1623/hysj.51.1.171, 2006.

Marsh, R., Müller, S. A., Yool, A., and Edwards, N. R.: Incorporation of the C-GOLDSTEIN efficient climate model into the GENIE framework: "eb_go_gs" configurations of GENIE, Geosci. Model Dev., 4, 957–992, doi:10.5194/gmd-4-957-2011, 2011.

Murphy, J. M., Booth, B. B. B., Collins, M., Harris, G. R., Sexton, D. M. H., and Webb, M. J.: A methodology for probabilistic predictions of regional climate change from perturbed physics ensembles, Phil. Trans. R. Soc. A, 365, 1993–2028, doi:10.1098/rsta.2007.2077, 2007.

Norby, R. J., DeLucia, E. H., Gielen, B., Calfapietra, C., Giardina, C. P., King, J. S., Ledford, J., McCarthy, H. R., Moore, D. J/P., Ceulemans, R., De Angelis, P., Finzi, A. C., Karnosky, D. F., Kubiske, M. E., Lukac, M., Pregizter, K. S., Scarascia-Mugnozza, G. E., Schlesinger, W. H., and Oren R.: Forest response to elevated CO_2 is conserved across a broad range of productivity, Proc. Natl. Acad. Sci. USA, 102, 18052–18056, doi:10.1073/pnas.0509478102, 2005.

Norby, R. J., Warren, J. M., Iversen, C. M., Garten, C. T., Medlyn, B. E., and McMurtrie, R. E.: CO_2 enhancement of forest productivity constrained by limited nitrogen availability, Proc. Natl. Acad. Sci. USA, 107, 19368–19373, doi:10.1073/pnas.1006463107, 2010.

Olofsson, J. and Hickler, T.: Effects of human land-use on the global carbon cycle during the last 6,000 years, Veg. Hist. Archaeobot., 17, 605–615, doi:10.1007/s00334-007-0126-6, 2008.

Pongratz, J., Reick, C., Raddatz, T., and Claussen, M.: A reconstruction of global agricultural areas and land cover for the last millennium, Global Biogeochem. Cy., 22, GB3018, doi:10.1029/2007GB003153, 2008.

Ridgwell, A. and Hargreaves, J.: Regulation of atmospheric CO_2 by deep-sea sediments in an Earth system model, Global Biogeochem. Cy., 21, GB2008, doi:10.1029/2006GB002764, 2007.

Ridgwell, A., Hargreaves, J. C., Edwards, N. R., Annan, J. D., Lenton, T. M., Marsh, R., Yool, A., and Watson, A.: Marine geochemical data assimilation in an efficient Earth System Model of global biogeochemical cycling, Biogeosciences, 4, 87–104, doi:10.5194/bg-4-87-2007, 2007.

Rougier, J.: Probabilistic inference for future climate using an ensemble of climate model evaluations, Climate Change, 82, 247–264, doi:10.1007/s10584-006-9156-9, 2007.

Sabine, C., Feely, R. A., Gruber, N., Key, R. M., Lee, K., Bullister, J. L., Wanninkhof, R., Wong, C. S., Wallace, D. W. R., Tilbrook, B., Millero, F. J., Peng, T.-H., Kozyr, A., Ono, T., and Rios, A. F.: The oceanic sink for anthropogenic CO_2, Science, 305, 367–371, doi:10.1126/science.1097403, 2004.

Discussion Paper | Discussion Paper | Discussion Paper | Discussion Paper |

BGD
9, 9425–9451, 2012

A model-based constraint of CO_2 fertilisation

P. B. Holden et al.

Smith, B., Prentice, I. C., and Sykes, M. T.: Representation of vegetation dynamics in the modelling of terrestrial ecosystems: comparing two contrasting approaches within European climate space, Global Ecol. Biogeogr., 10, 621–637, doi:10.1046/j.1466-822X.2001.t01-1-00256.x, 2001.

Stocker, B. D., Strassmann, K., and Joos, F.: Sensitivity of Holocene atmospheric CO_2 and the modern carbon budget to early human land use: analyses with a process-based model, Biogeosciences, 8, 69–88, doi:10.5194/bg-8-69-2011, 2011.

Waha, K., van Bussel, L. G. J., Müller, C., and Bondeau, A.: Climate-driven simulation of global crop sowing dates, Global Ecol. Biogeogr., 21, 247–259, doi:10.1111/j.1466-8238.2011.00678.x, 2012.

Williamson, M. S., Lenton, T. M., Shepherd, J. G., and Edwards, N. R.: An efficient numerical terrestrial scheme (ENTS) for Earth system modelling, Ecol. Modell., 198, 362–374, doi:10.1016/j.ecolmodel.2006.05.027, 2006.

BGD
9, 9425–9451, 2012

Table 1. Ensemble design (Sect. 3). Four ensembles were performed, each varying 4 uncalibrated parameters between the tabulated ranges. Experiments 1, 3 and 4 were 100-member ensembles with the same randomly selected sub-sample of the 471-member spin-ups. Experiment 2 was performed on the remaining 371 spin-ups. Experiment 1 applied a more conservative range for ALUA. Experiments 3 and 4 were performed to better calibrate the tails of the VPC distribution.

Parameter code (GENIE variable)	Range	Distribution	Description
OL1(olr_adj)	-0.5 to $0.5\,\mathrm{W\,m^{-2}}$	Linear	Outgoing Longwave Feedback; Holden et al. (2010)
VPC (k14)	1. 30 to 700 ppm 2. 30 to 700 ppm 3. 0 to 30 ppm 4. 650 to 850 ppm	1. Logarithmic 2. Logarithmic 3. Linear 4. Linear	Michaelis-Menten saturation of CO_2 fertilisation Williamson et al. (2006)
KC (kc)	0.0 to 1.0	Linear	Reduction of leaf-litter input to soils under Land Use Change Eq. (3)
ALUA (albcavg)	1. 0.14 to 0.16 2. 0.12 to 0.18 3. 0.12 to 0.18 4. 0.12 to 0.18	Linear	Crop albedo Eq. (6)

BGD
9, 9425–9451, 2012

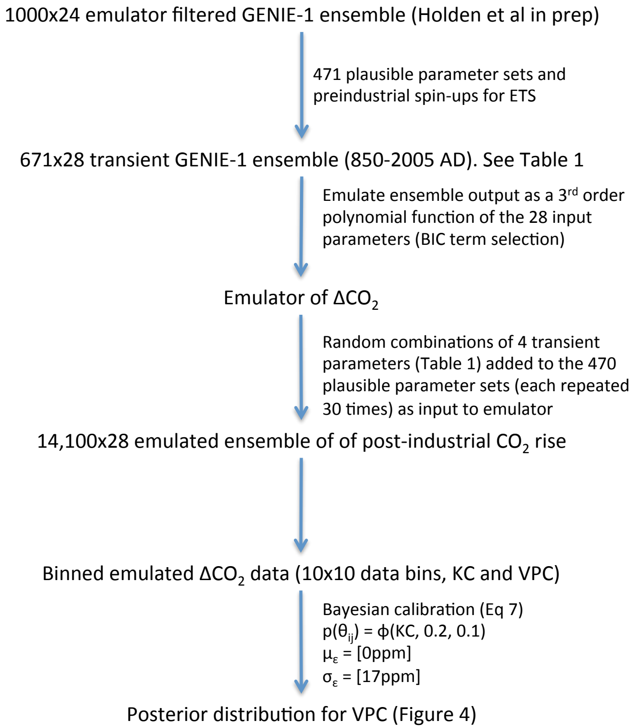

Fig. 1. Flow chart describing the experimental design.

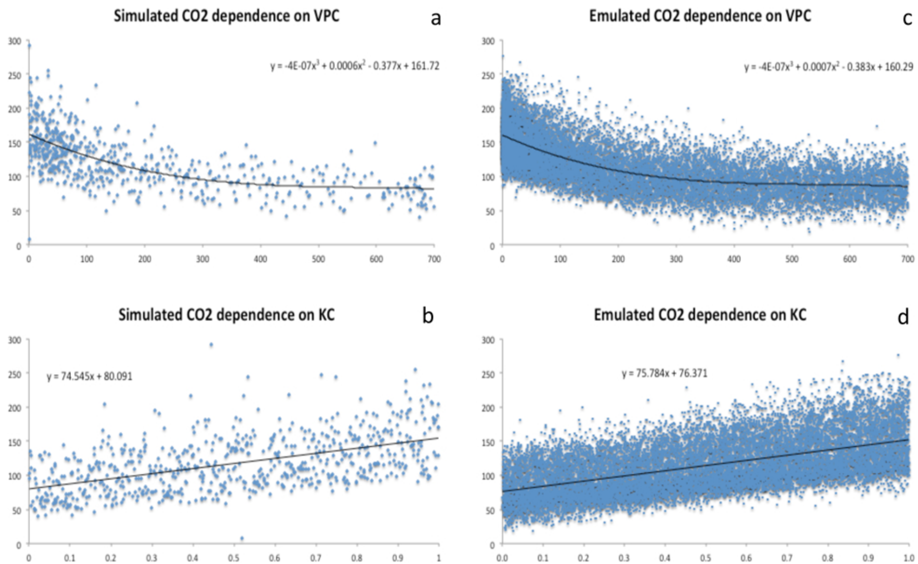

Fig. 2. Simulated CO_2 dependence upon **(a)** VPC and **(b)** KC compared with the emulated CO_2 dependencies on **(c)** VPC and **(d)** KC.

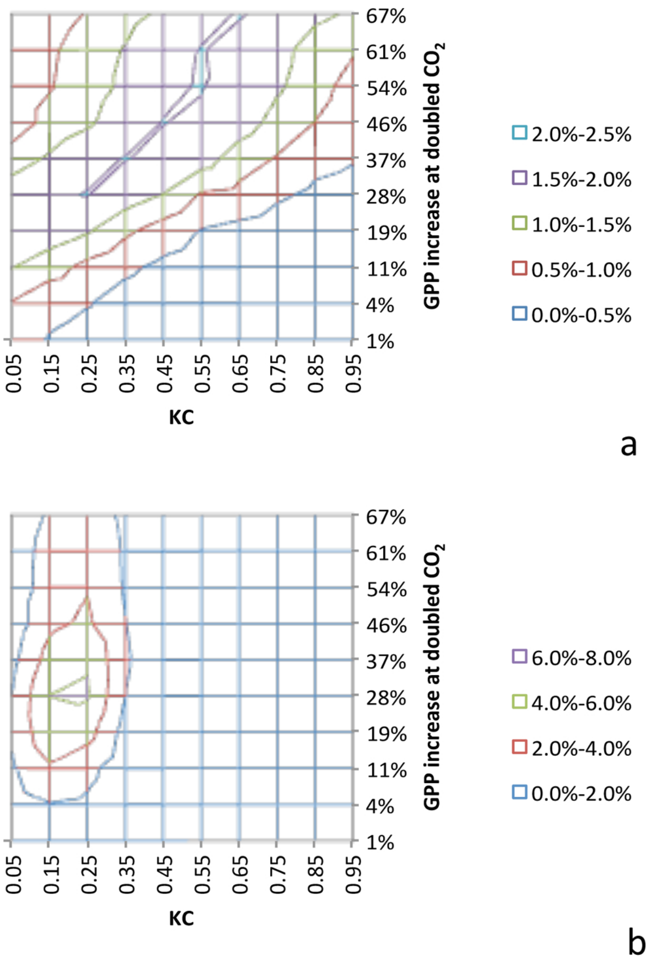

Fig. 3. Joint probability distributions for KC and VPC, applying Eq. (7) with **(a)** a uniform prior distribution $p(\theta_{ij}) = 1$ and **(b)** a prior assumption for KC, $p(\theta_{ij}) = \varphi$ (KC, 0.2, 0.1).

BGD
9, 9425–9451, 2012

A model-based constraint of CO_2 fertilisation

P. B. Holden et al.

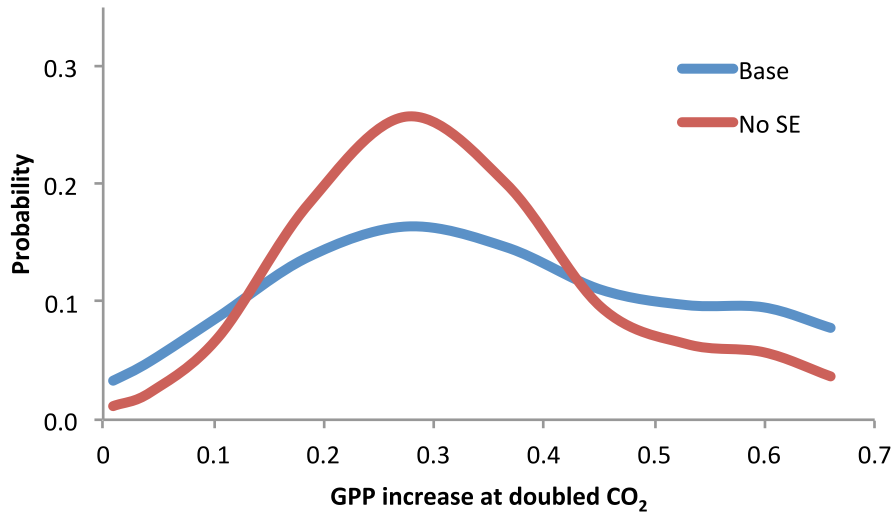

Fig. 4. Marginal probability distribution for the GPP increase in response to a doubling of CO_2 calculated (red) neglecting structural error and (blue) allowing for structural error, estimated from the uncertainty exhibited in an inter-model comparison (see Sect. 4). Although structural error is often neglected in studies of this type, the neglect leads to an unreasonably precise calibration, being effectively equivalent to the assumption that the model is perfect.

BGD
9, 9425–9451, 2012

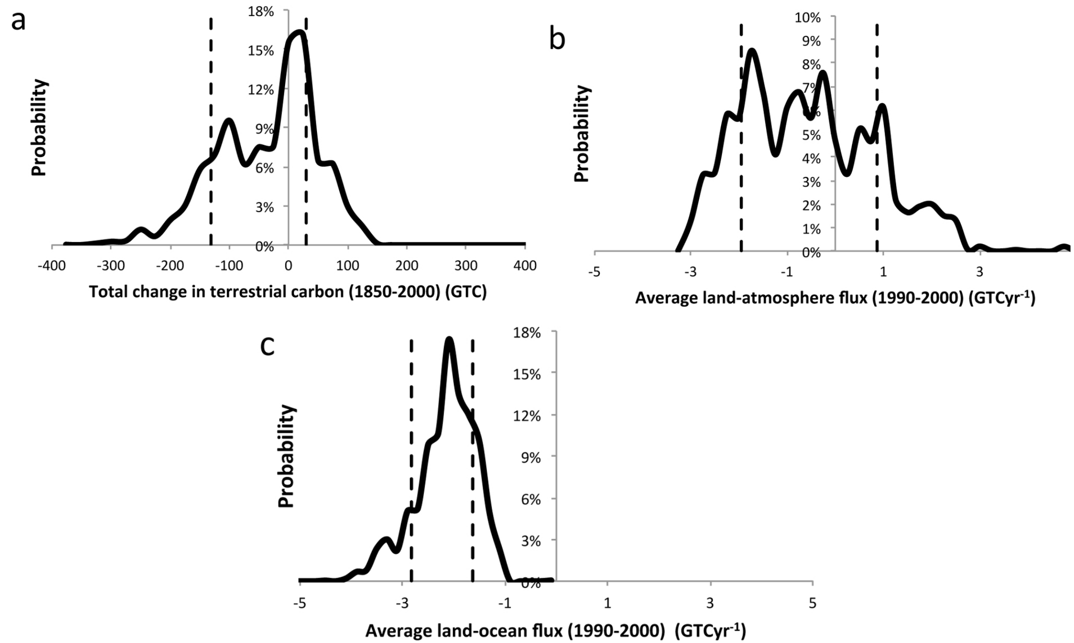

Fig. 5. Probability distributions of carbon exchange between land-atmosphere-ocean. Each calculation applies the prior distribution for KC, $p(\theta_{ij}) = \varphi$ (KC, 0.2, 0.1), together with the posterior distribution for VFC (blue curve, Fig. 4) to probability weight each of the 670 GENIE simulations. Distributions are **(a)** change in terrestrial carbon over the post-industrial period (1850 to 2000), **(b)** annually-averaged land-atmosphere flux (1990 to 2000) and **(c)** annually-averaged ocean-atmosphere flux (1990 to 2000). Vertical dashed lines illustrate the 66 % confidence interval.

BGD
9, 9425–9451, 2012

A model-based constraint of CO_2 fertilisation

P. B. Holden et al.